Self-diffusion of rodlike molecules in strong shear fields

Sten Sarman, Peter J. Daivis, and Denis J. Evans
Research School of Chemistry, Australian National University, Canberra, Australian Capital Territory, 2601 Australia
(Received 21 September 1992)

We apply recently derived Green-Kubo relations for the various elements of the self-diffusion tensor (SDT) of shearing fluids to three different model systems of rodlike molecules: the Tildesley-Madden model for carbon disulfide, the Gay-Berne fluid, and the Ryckaert-Bellemans model for decane. We study how the various elements of the SDT depend on the shear rate. This dependence is explained in greater detail by examining the various velocity autocorrelation functions, the order parameter, and the shear induced rotation rate. We find that two different mechanisms are responsible for the behavior of the diagonal elements of the SDT. The first is the elliptical distortion of the nearest-neighbor shell and enhances the diagonal elements of the SDT. The second is the shear alignment of the molecules. This facilitates diffusion in the alignment direction and suppresses diffusion in the perpendicular direction. We also suggest "collision" sequences that are responsible for the sign of the off-diagonal elements of the SDT.

PACS number(s): 03.40.Gc, 02.50.−r, 51.10.+y

I. INTRODUCTION

When a fluid is subject to a weak shear field, Curie's principle of linear irreversible thermodynamics [1] states that a planar shear, being a second-rank tensor, cannot generate mass or heat currents which are polar vectors. However, when the shear rate increases, nonlinear effects become important and Curie's principle breaks down. Then it is still impossible for a shear field to generate a mass current or a heat flow but it can modify the thermal conductivity and the diffusion coefficient. These coefficients then become second-rank tensors with shear rate dependent elements.

At equilibrium these two transport coefficients can be calculated microscopically in several different ways. The most straightforward method is to perform an equilibrium molecular-dynamics (EMD) simulation where the Green-Kubo integrals of the heat current or mass current autocorrelation functions are calculated from a single molecular-dynamics simulation. In the case of self-diffusion there is also a well-known relation between the mean-square displacements (MSD) and the self-diffusion coefficient. Another method is to perform nonequilibrium molecular-dynamics (NEMD) simulations. Then an external field, driving an irreversible mass or heat current, is coupled to the system. The functional form of the field is chosen in such away that the current generated is exactly the same as that induced by a chemical potential or temperature gradient, respectively. By using linear response theory one can prove that the transport coefficient in question is obtained as the ratio of the current to the field in the zero-field limit [2].

The first attempt to extend these methods to shearing fluids was made by Heyes *et al.* [3]. These authors postulated without proof expressions for the relations between the diagonal elements of the self-diffusion tensor (SDT) and the mean-square displacements.

In a series of papers [4–8] we have generalized and proved the above expressions for fluids subject to strong shear. We have derived Green-Kubo (GK) formulas for diagonal and off-diagonal elements of the thermal conductivity and mutual diffusion tensors and we have proved the relations between the MSD and the various elements of the SDT. It might be reasonable to believe that since there are GK integrals for the above-mentioned quantities it should be a simple matter to generalize the NEMD methods to strongly shearing fluids. Unfortunately, it has been shown that this is not the case [7]. There are *no* simple efficient NEMD algorithms for the shear dependent thermal conductivity or the shear dependent self- or mutual-diffusion tensors.

In Ref. [8] we applied the GK expressions to calculate the SDT of a shearing Lennard-Jones fluid. We found that, at the triple point, the diagonal elements of the SDT increase by a factor of 2 when the reduced shear rate was unity. (NB, reduced quantities are defined in Sec. II.) The off-diagonal elements were found to be at least three orders of magnitude smaller than the diagonal elements and it was impossible to determine their sign. At lower densities and higher temperatures the diagonal elements of the SDT were less affected by the shear field. However, the off-diagonal elements were found to increase significantly with the shear rate and at reduced shear rates of unity they were of the same magnitude as the diagonal ones.

In this paper we have chosen to extend the previous study to fluids consisting of rodlike molecules, where the effect of the shear field upon diffusion can be expected to be larger because of the alignment of the molecules caused by the presence of the shear. In particular, we have chosen to examine three different systems: carbon disulfide, the Gay-Berne (GB) fluid [9], and decane. The CS_2 molecules have been modeled as three fused Lennard-Jones (LJ) spheres [10]. The length to width ratio is about 2:1. The GB fluid simulated here can, loosely speaking, be regarded as LJ ellipsoids with a length to width ratio of 3:1. For decane we studied a model similar to the Ryckaert-Bellemans model [11]. Unlike the other

two molecules, this molecule is flexible.

The paper is organized as follows; in Sec. II we review the necessary theory and describe the various models, in Sec. III the results are presented and discussed, and finally in Sec. IV there is a conclusion.

II. THEORY AND METHOD

A. Model fluids

Since the effect of a shear field upon diffusion of fluids consisting of spherical molecules was found to be small [4,8] we believe that larger effects can be found if the fluid consists of molecules that are more anisotropic. Therefore, we have turned our attention to three models for rodlike and flexible molecules: the Tildesley-Madden (TM) model of carbon disulfide [10], the Gay-Berne [9] fluid, and the Ryckaert-Bellemans (RB) [11] model of decane.

The TM model of carbon disulfide is a rigid three-center interaction site model, where the different sites interact according to a Lennard-Jones potential,

$$u_{\mathrm{LJ}\mu\nu}=4\varepsilon_{\mu\nu}\left[\frac{\sigma_{\mu\nu}^{12}}{r^{12}}-\frac{\sigma_{\mu\nu}^{6}}{r^{6}}\right], \tag{2.1}$$

where $\sigma_{\mu\nu}$ is the zero of the potential and $\varepsilon_{\mu\nu}$ is the depth of the minimum. The carbon–sulfur bond length is 1.57 Å. The values of the different potential parameters are $\sigma_{\mathrm{CC}}=3.35$ Å, $\sigma_{\mathrm{CS}}=3.44$ Å, $\sigma_{\mathrm{SS}}=3.52$ Å, $\varepsilon_{\mathrm{CC}}/k_B=51.2$ K, $\varepsilon_{\mathrm{CS}}/k_B=96.80$ K, and $\varepsilon_{\mathrm{SS}}/k_B=183.00$ K, where k_B is Boltzmann's constant. The cutoff distance between a site of a species μ and a site of a species ν has been set to $r_{c\mu\nu}=2.5\sigma_{\mu\nu}$, i.e., the cutoff distance is slightly different for different kinds of interactions. The length to width ratio of this molecule is roughly equal to 2:1. The numerical results obtained for CS_2 are given in reduced units. The length unit is σ_{CC}, the mass unit is $m_{\mathrm{C}}=12.00$ amu, the energy unit is $\varepsilon_{\mathrm{CC}}$ and the time unit $\tau=\sigma_{\mathrm{CC}}(m_{\mathrm{C}}/\varepsilon_{\mathrm{CC}})^{1/2}\approx 1.8$ ps. We have chosen to simulate the triple point where the density and temperatures are equal to 1.55 g cm^{-3} and 163 K. In reduced units this becomes $n\sigma_{\mathrm{CC}}^3=0.461\,81$ and $kT_B/\varepsilon_{\mathrm{CC}}=3.1836$. The equations of motion were integrated by a fourth-order Gear predictor corrector method with a time step of 0.002τ for reduced shear rates, $\gamma\tau$, less than 0.50 and 0.001τ for the higher shear rates. The run lengths were 1000τ.

A Gay-Berne fluid consists of molecules shaped like ellipsoids of revolution, which interact according to the following pair potential:

$$U_{\mathrm{GB}}(\mathbf{r}_{12},\hat{\mathbf{u}}_1,\hat{\mathbf{u}}_2)=4\varepsilon(\hat{\mathbf{r}}_{12},\hat{\mathbf{u}}_1,\hat{\mathbf{u}}_2)\left\{\left[\frac{\sigma_0}{r_{12}-\sigma(\hat{\mathbf{r}}_{12},\hat{\mathbf{u}}_1,\hat{\mathbf{u}}_2)+\sigma_0}\right]^{12}-\left[\frac{\sigma_0}{r_{12}-\sigma(\hat{\mathbf{r}}_{12},\hat{\mathbf{u}}_1,\hat{\mathbf{u}}_2)+\sigma_0}\right]^{6}\right\}, \tag{2.2a}$$

where $\hat{\mathbf{u}}_1$ and $\hat{\mathbf{u}}_2$ are unit vectors along the axis of revolution of molecules 1 and 2, $\mathbf{r}_{12}$ is the unit vector in the direction of the distance vector $\mathbf{r}_{12}=\mathbf{r}_2-\mathbf{r}_1$ between the centers of molecules 1 and 2, and r_{12} is the scalar distance between them.

The strength parameter $\varepsilon(\mathbf{r}_{12},\hat{\mathbf{u}}_1,\hat{\mathbf{u}}_2)$ and the range parameter $\sigma(\hat{\mathbf{r}}_{12},\hat{\mathbf{u}}_1,\hat{\mathbf{u}}_2)$ are given by

$$\varepsilon(\hat{\mathbf{r}}_{12},\hat{\mathbf{u}}_1,\hat{\mathbf{u}}_2)=\varepsilon_0[1-\chi^2\hat{\mathbf{u}}_1\cdot\hat{\mathbf{u}}_2]^{-1/2}\times\left\{1-\frac{\chi'}{2}\left[\frac{(\hat{\mathbf{r}}_{12}\cdot\hat{\mathbf{u}}_1+\hat{\mathbf{r}}_{12}\cdot\hat{\mathbf{u}}_2)^2}{1+\chi'\hat{\mathbf{u}}_1\cdot\hat{\mathbf{u}}_2}-\frac{(\hat{\mathbf{r}}_{12}\cdot\hat{\mathbf{u}}_1-\hat{\mathbf{r}}_{12}\cdot\hat{\mathbf{u}}_2)^2}{1-\chi'\hat{\mathbf{u}}_1\cdot\hat{\mathbf{u}}_2}\right]\right\}^2 \tag{2.2b}$$

and

$$\sigma(\hat{\mathbf{r}}_{12},\hat{\mathbf{u}}_1,\hat{\mathbf{u}}_2)=\sigma_0\left\{1-\frac{\chi}{2}\left[\frac{(\hat{\mathbf{r}}_{12}\cdot\hat{\mathbf{u}}_1+\hat{\mathbf{r}}_{12}\cdot\hat{\mathbf{u}}_2)^2}{1+\chi\hat{\mathbf{u}}_1\cdot\hat{\mathbf{u}}_2}-\frac{(\hat{\mathbf{r}}_{12}\cdot\hat{\mathbf{u}}_1-\hat{\mathbf{r}}_{12}\cdot\hat{\mathbf{u}}_2)^2}{1-\chi\hat{\mathbf{u}}_1\cdot\hat{\mathbf{u}}_2}\right]\right\}^{-1/2}, \tag{2.2c}$$

with $\chi=(\kappa^2-1)/(\kappa^2+1)$, where κ is the ratio of the semiaxis in the direction of the axis of revolution and the other semiaxis, i.e., the length to breadth ratio for a prolate ellipsoid of revolution. The parameter $\chi'=(\kappa'^{1/2}-1)/(\kappa'^{1/2}+1)$, where κ' is the ratio of potential well depths for the side by side configuration and the end to end configuration. In this work we have used the value 3.00 for κ and 5.00 for κ'. The simulation results for this model are given in length, energy mass, and time units of σ_0, ε_0, m, and $\tau=\sigma_0(m/\varepsilon_0)^{1/2}$. The moment of inertia about the axis of revolution is equal to zero. The moment of inertia about the two axes perpendicular to the axis of revolution has been given the value $m\sigma_0^2$, i.e., unity in reduced units. The equations of motion have been integrated by a fourth-order Gear predictor corrector algorithm with a time step of 0.001τ. The run lengths were 500τ. All simulation data reported for the GB fluid in this work are for a reduced density $n\sigma_0^3$ of 0.30 and reduced temperature k_BT/ε_0 of 1.25, except for the data in Fig. 9 where the reduced density is 0.10 and the reduced temperature is 1.25. The high density state point is just below the isotropic liquid–nematic liquid crystal-phase transition. The equilibrium properties of this fluid have been comprehensively studied by de Miguel, Rull, Gubbins, and co-workers [12–15].

The rotational part of the equations of motion for these two model systems was expressed in terms of quaternions [16].

The equations of motion for the centers of mass were the Sllod equations [2]

$$\dot{\mathbf{r}}_i=\frac{\mathbf{p}_i}{m}+\mathbf{n}_x\gamma y_i \tag{2.3a}$$

and

$$\dot{\mathbf{p}}_i = F_i - \mathbf{n}_x \gamma p_{yi} - \alpha \mathbf{p}_i \ . \tag{2.3b}$$

In the above equations $\mathbf{r}_i$ is the laboratory position of the center of mass of molecule i, $\mathbf{F}_i$ is the intermolecular force on molecule i due to the other molecules, and $\mathbf{n}_x$ is the unit vector in the x direction. At low Reynolds numbers, the only nonzero component of the streaming velocity is the x component, u_x, which is equal to $\mathbf{n}_x \gamma y$ (i.e., there is a velocity gradient in the y direction). Consequently, the only nonzero element in the shear rate tensor is $\partial u_x / \partial y = \gamma$. The streaming velocity at the position of the center of gravity of molecule is $\mathbf{n}_x \gamma y_i$, so the peculiar translational velocity of the center of gravity of the molecule is $\mathbf{p}_i / m$.

The Gaussian thermostatting multiplier, α, is determined by making the peculiar translational kinetic energy a constant of motion,

$$\alpha = \frac{\sum_{i=1}^{N} [\mathbf{F}_i \cdot \mathbf{p}_i - \gamma p_{xi} p_{yi}]}{\sum_{i=1}^{N} \mathbf{p}_i^2} \ . \tag{2.4}$$

The model used for the simulation of decane is a simplification of the Ryckaert-Bellemans [11] model for n alkanes. The model alkane molecules are composed of sites representing the CH_2 or CH_3 groups of the n alkane. For simplicity we assume that all sites have the same mass, 14.52 amu. The distance between neighboring sites (the bond length) is fixed at 1.53 Å and the bond angles are fixed at 109.47°, using a next-nearest-neighbor distance constraint. The freezing out of the high-frequency modes associated with bond vibration and libration enables the use of much larger integration time steps than would otherwise be possible, but gives slightly different results than would be obtained for a model allowing bond angle bending. A torsional or dihedral potential acts between each pair of methyl or methylene groups that are three bonds apart on a given n-alkane chain. To model this we use a potential function that depends on the dihedral angle ϕ, where $\cos\phi = -(\mathbf{r}_i \times \mathbf{r}_{i+1}) \cdot (\mathbf{r}_{i+1} \times \mathbf{r}_{i+2})$ and $\mathbf{r}_i, \mathbf{r}_{i+1}$, and $\mathbf{r}_{i+2}$ are successive bond vectors. Following Ryckaert and Bellemans we use a truncated power series in the cosine of ϕ for the dihedral potential,

$$\Phi_{\text{dihedral}}(\phi)/k_B = \sum_{i=0}^{5} a_i \cos^i(\phi) \ , \tag{2.5}$$

where values of the coefficients $\{a_i\}$ are given by {1116 K, 1462 K, −1578 K, −368 K, 3156 K, −3788 K}. Sites on different molecules, and sites more than three bonds apart on the same molecule, interact through a modified 12-6 Lennard-Jones potential,

$$\Phi_{\text{LJ}} = \begin{cases} 4\varepsilon \left[\left(\dfrac{\sigma}{r} \right)^{12} - \left(\dfrac{\sigma}{r} \right)^{6} \right] + \varepsilon \ , & r < 2^{1/6}\sigma \ , \\ 0 \ , & r \geq 2^{1/6}\sigma \ , \end{cases} \tag{2.6}$$

with parameters $\sigma = 3.923$ Å and $\varepsilon/k_B = 72$ K. In contrast to the original RB model our Lennard-Jones potential has been truncated at its minimum $r/\sigma = 2^{1/6}$, and shifted by ε so that the potential is zero at the point of truncation (this also ensures that the force is zero at the cutoff distance, $r/\sigma = 2^{1/6}$). This potential, often referred to as the WCA potential, has no attractive part and is short ranged, making it convenient from the computational point of view since the number of interacting neighbors is reduced. This model is useful for examining the qualitative behavior of flexible versus rigid molecules, but it is not expected to give quantitative agreement with experimental results.

The molecular version of the Sllod algorithm [2] (so named because of its close relationship with the Dolls tensor algorithm) given by Edberg, Evans, and Morriss [17] was used for the decane simulations. The number of molecules, the kinetic temperature, the volume, and the total momentum were all fixed. The equations of motion for site α of molecule i are given by

$$\dot{\mathbf{r}}_{i\alpha} = \frac{\mathbf{p}_{i\alpha}}{m_\alpha} + \mathbf{n}_x \gamma y_i \tag{2.7a}$$

and

$$\dot{\mathbf{p}}_{i\alpha} = \mathbf{F}_{i\alpha}^{N} + \mathbf{F}_{i\alpha}^{C} - \frac{m_\alpha}{M_i} \mathbf{n}_x \gamma p_{yi} - \frac{m_\alpha}{M_i} \alpha \mathbf{p}_i \ , \tag{2.7b}$$

where $\mathbf{F}^N$ represents the force due to dihedral and Lennard-Jones potentials, and $\mathbf{F}^C$ represents the intramolecular constraint forces. In these equations, m_α is the mass of site α, M_i is the mass of molecule i, $\mathbf{n}_x$ is the unit vector in the x direction, γ is the shear rate, $\mathbf{p}_i$ is the peculiar momentum of the center of mass of molecule i, and α is the thermostatting multiplier (which should not be confused with the site index, α). The thermostat keeps the molecular translational (or center-of-mass) kinetic temperature fixed, so that

$$\alpha = \frac{\sum_{i=1}^{N} \frac{1}{M_i} \{\mathbf{F}_i \cdot \mathbf{p}_i - \gamma p_{xi} p_{yi}\}}{\sum_{i=1}^{N} \frac{1}{M_i} \mathbf{p}_i^2} \ . \tag{2.8}$$

All results for decane are reported in units reduced with respect to the alkyl group Lennard-Jones potential parameters ε and σ and the alkyl group mass, m. The time unit, τ, is equal to $\sigma(m/\varepsilon)^{1/2}$. More detailed descriptions of the equations of motion and the simulation technique, including the Gaussian constraint method, can be found in the Refs. [17,18]. The state point we have chosen to simulate has a density and temperature of 0.730 g cm^{-3} and 293 K, corresponding to reduced density $\rho_m \sigma^3 = 0.183$ and temperature $k_B T/\varepsilon = 4.07$. The run lengths were 150τ and the time step was 0.001τ.

B. Theory

When a one-component fluid is subject to strong shear, the self-diffusion coefficient becomes a second-rank tensor with shear rate dependent components. If the shear rate γ is given by $\gamma = \partial u_x / \partial y$, where u_x is the streaming velocity in the x direction, the representation of the self-diffusion tensor in Cartesian coordinates becomes

$$\mathbf{D}=\begin{bmatrix} D_{xx} & D_{xy} & 0 \\ D_{yx} & D_{yy} & 0 \\ 0 & 0 & D_{zz} \end{bmatrix} . \tag{2.9}$$

The xz, yz, zx, and zy elements are identically zero by symmetry. In previous work [6] the following Green-Kubo relations for the various components of this tensor were derived:

$$D_{\alpha\beta}=\frac{1}{m^2}\int_0^\infty \langle p_{i\alpha}(t)p_{i\beta}(0)\rangle_\gamma dt$$
$$=\int_0^\infty \langle v_{i\alpha}(t)v_{i\beta}(0)\rangle_\gamma dt \quad \forall i=1,N , \tag{2.10}$$

where $\alpha,\beta=x,y,z$. The average $\langle\ \rangle$ is a time average taken over a shearing steady state, hence the subscript γ. Note that the $p_{i\alpha}$ in this equation are components of the peculiar momenta of the molecular centers of mass and that the velocities $v_{i\alpha}=p_{i\alpha}/m$, where m is the molecular mass, are peculiar velocities. These relations can be integrated giving Einstein relations for the mean-square displacement at long times. The diagonal components become

$$\lim_{t\to\infty}\langle q_{i\alpha}(t)^2\rangle_\gamma=2D_{\alpha\alpha}t \quad \forall i=1,N , \tag{2.11}$$

where

$$\mathbf{q}_i(t)\equiv\mathbf{r}_i(0)+\int_0^t ds\frac{\mathbf{p}_i(s)}{m} \tag{2.12}$$

is the convected, Lagrangian, position of particle i. It is not possible to obtain separate Einstein relations for the two nonzero off-diagonal elements of the diffusion tensor [5]. It is only possible to obtain an Einstein relation for the sum of these two elements,

$$\lim_{t\to\infty}\langle q_{ix}(t)q_{iy}(t)\rangle_\gamma=(D_{xy}+D_{yx})t \quad \forall i=1,N . \tag{2.13}$$

All of the values of the diffusion coefficients reported here have been obtained by computing the Green-Kubo integrals, Eq. (2.10). In some cases we have evaluated the MSD expressions as a cross-check. Then the GK values and the MSD values have always been found to agree within the statistical uncertainty.

A useful quantity when one deals with anisotropic molecules is the symmetric traceless order tensor,

$$\mathbf{S}=\frac{3}{2}\left[\frac{1}{N}\sum_{i=1}^{N}\hat{\mathbf{u}}_i\hat{\mathbf{u}}_i-\frac{1}{3}\mathbf{1}\right] . \tag{2.14}$$

The unit vector $\hat{\mathbf{u}}_i$ is parallel to the axis of revolution of the GB or CS_2 molecules or the eigenvector corresponding to the largest eigenvalue of the averaged inertial ellipsoid of the decane molecule. The largest eigenvalue of the order tensor will be denoted by S. When the orientation of the molecules is random, S is zero, and when they are perfectly aligned S is unity. The eigenvector corresponding to S is called the director and it can be interpreted as the preferred alignment direction of the molecules. The angle between the streamlines and the director is known as the alignment angle. In the linear regime molecules align themselves at 45° to the streamlines. In the simulations in this work we are mainly in the nonlinear regime and here the alignment angle is less than 45°.

The following discussion will involve the traceless symmetric parts of the pressure tensor and the SDT. We will also refer to the angle between the eigenvector corresponding to the largest eigenvalue of these two tensors and the streamlines as alignment angles.

Linear irreversible thermodynamics predicts that molecules in a homogeneous fluid under steady shear rotate at an average angular velocity equal to half the vorticity, i.e.,

$$\langle\boldsymbol{\omega}\rangle=\tfrac{1}{2}\nabla\times\mathbf{u} , \tag{2.15}$$

where $\mathbf{u}$ is the steaming velocity. Therefore the average angular velocity in simple shear flow becomes $\langle\boldsymbol{\omega}\rangle=-\gamma\mathbf{n}_z/2$, where $\mathbf{n}_z$ is the unit vector in the z direction. In the nonlinear regime it has been found that the rotation rate is lower than $\gamma/2$ [19,20]. It is reasonable to assume that the rotation period of the molecules should be of the same order as the decay time of the velocity autocorrelation functions in order to affect diffusion.

III. RESULTS AND DISCUSSION

The first system that we examined was carbon disulfide at its triple point. The diagonal elements of the SDT as a function of shear rate are depicted in Fig. 1. As one can see, they increase dramatically with γ up to $\gamma\tau=1.0$. Then they level off or decrease again. For shear rates greater than 3 a string phase forms [2]. The ratio between the maximum of the xx element of the SDT and the equilibrium value is about 40 which is much larger than the corresponding ratio for a LJ fluid at the triple point, namely, about 2. Part of the reason for this is that the equilibrium diffusion coefficient of CS_2 at the triple point is very low. It is about 10 times smaller than the diffusion coefficient of a LJ fluid at its triple point.

In order to understand why the diffusion coefficient increases so dramatically one can study the velocity autocorrelation functions (VACF). If we look at the VACF of the dense equilibrium fluid, Fig. 2, we find that it consists

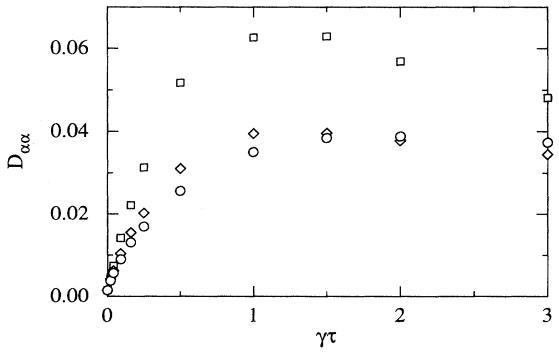

FIG. 1. The diagonal elements of the SDT of CS_2 as a function of the shear rate. The open squares, the open diamonds, and the open circles depict D_{xx}, D_{yy}, and D_{zz}, respectively.

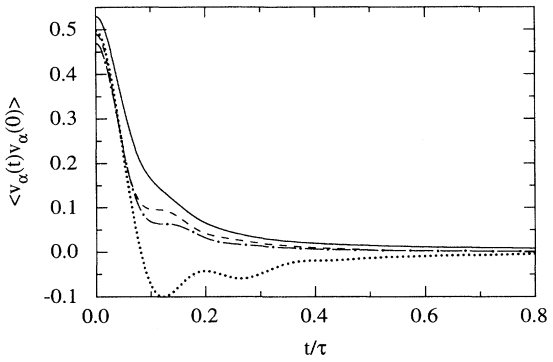

FIG. 2. Diagonal velocity autocorrelation functions, $Z_{\alpha\alpha}(t)=\langle v_\alpha(t)v_\alpha(0)\rangle$ of CS_2. The full curve, the dashed curve, and the dash-dotted curve denote $Z_{xx}(t)$, $Z_{yy}(t)$, and $Z_{zz}(t)$ at a reduced shear rate of 1.0. The dotted curve is the equilibrium velocity autocorrelation function.

of a positive region immediately followed by a negative area. This negative region is due to rebounds when a molecule collides with its nearest neighbors. If one integrates this function with respect to time the negative contribution almost cancels the positive contribution so the resulting diffusion coefficient is very small. When we study the VACF for the diagonal elements of the SDT at high shear rates we find that the negative rebound area has vanished and that the initial positive part of the VACF remains positive for a longer time than at equilibrium. This leads to a sharp increase of the magnitude of the time integral of the VACF and thereby the diagonal elements of the SDT. This is basically the same mechanism that enhances the diffusion in a Lennard-Jones fluid under shear [4,8].

Another important phenomenon that affects diffusion is the alignment of the molecules relative to the streamlines. The alignment angle of the order tensor decreases very rapidly with the shear rate. At $\gamma\tau=0.25$ it has fallen from the linear value of 45° to about 25°. It then stays at this value at least up to a reduced shear rate of 3.0. The order parameter, which is shown in Fig. 3(a), also increases very steeply to about 0.40. The high degree of ordering and the small alignment angle favor diffusion in the x direction, i.e., in the direction closest to the direction of the streamlines, at the expense of the z and y directions.

An interesting question is whether the SDT, which is a second-rank tensor, is correlated with any of the other second-rank tensors in the system, such as the pressure tensor or the order tensor. In order to answer this question we have compared their alignment angles. We have found that the alignment angles of the SDT and the order tensor are fairly well correlated for $\gamma\tau<1.0$. The behavior of the alignment angle of the pressure tensor, which can be seen in Fig. 3(b), is different. (We have only displayed the alignment angles of the SDT, the order tensor, and the pressure tensor of decane. However, the behavior of the alignment angles of these tensors in the GB fluid and CS_2 is similar.)

In the case of CS_2 the shear alignment is probably less

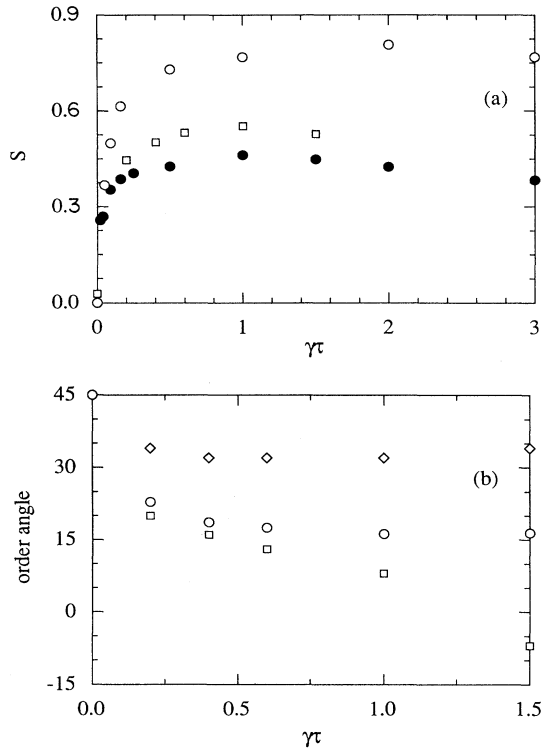

FIG. 3(a). The order parameter S as a function of the shear rate for the three different systems discussed in this work. The open circles, the open squares, and the filled circles represent the GB fluid, decane, and CS_2, respectively. (b) The alignment angle of various second-order symmetric traceless tensors in decane. The diamonds, the circles, and the squares depict the alignment angles of the pressure tensor, order tensor, and the traceless symmetric part of the SDT.

important than the distortion of the coordination shell and the eradication of the rebound region of the VACF. The leveling off and decrease of the diagonal elements of the SDT for reduced shear rates greater than 1.0 is due to the decrease of the initial positive region of the VACF. This is to a smaller extent due to increased pressure and to a larger extent due to the increased rotational temperature. Note that some caution is appropriate here. Up to a reduced shear rate of approximately 1.0 the equipartition principle is roughly valid. This means that the system properties are largely independent of the details of the thermostatting mechanism [21]. The fact that we only thermostat the molecular translational degrees of freedom consequently has little effect. For higher shear rates this is no longer true so the properties become dependent on the nature of the thermostat.

A relevant question to ask is to what extent does the shear induced rotation affect the VACF's? At a reduced shear rate of unity this period is equal to 45τ. This is much longer than the decay time of VACF's, which is about 1.0τ. It is thus reasonable to expect that the influence of the shear induced rotation upon the diffusion is very small.

The diagonal elements of the SDT of the GB fluid are displayed in Fig. 4. The xx element increases sharply at

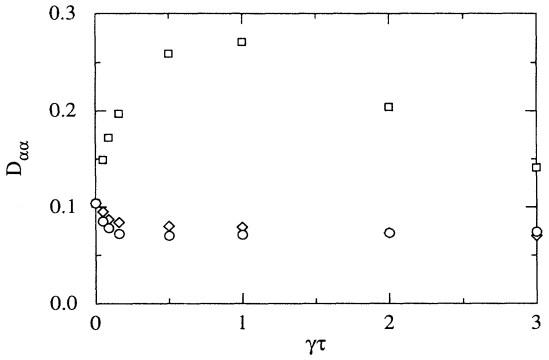

FIG. 4. As in Fig. 1 but the system is the GB fluid.

low shear rates and reaches a maximum at a reduced shear rate of 1.0, after which it diminishes again. The *yy* and the *zz* elements decrease monotonically with γ. This is in marked contrast to CS_2 where all the elements increase with γ. The rise of D_{xx} is strongly correlated with the rise of the order parameter, which is displayed in Fig. 3(a), and the fall of the alignment angle of the order tensor. At $\gamma\tau=0.15$ it has fallen to about 20°. After this it remains constant at this value, at least for $\gamma\tau<3.0$. As in CS_2, the alignment angles of the order tensor and the SDT are fairly well correlated, but the alignment angle of the pressure tensor is different. In the GB fluid alignment accounts for most of the shear induced changes in the SDT. This conclusion can be motivated by studying the VACF's at various shear rates. The diagonal VACF's of the GB fluid are shown in Fig. 5. At equilibrium the VACF decays almost monotonically to zero without any negative backscattering regions. This is probably due to the ease with which elongated molecules can break through any nearest-neighbor cage. At a reduced shear rate of 1.0, the decay time of the *xx* VACF has increased markedly. This longer decay time causes an increase of D_{xx}. On the other hand, the decay times of the *yy* and *zz* VACF's decrease and features of backscattering become apparent, both of which contribute to the reduction of D_{yy} and D_{zz}. This behavior is not unreasonable, because when the molecules are aligned almost parallel to the *x* axis and the streamlines, the molecules have to move sideways if they are to move in the *y* or *z* direction. At higher shear rates D_{xx} falls off again. This coincides with a rise in the rotational kinetic energy due to higher instantaneous angular velocities around the *y* axis and the *z* axis. Both of these rotational modes are likely to impede diffusion in the *x* direction. As mentioned before, the distribution of kinetic energy between various degrees of freedom at high shear rates depends on the thermostatting mechanism and it is very likely that other mechanisms would produce different results when $\gamma\tau\geq 1.0$.

The shortest average shear induced rotation period is about 250τ, even at the highest shear rates. This is far longer than the decay time of the VACF's. One can thus expect that the influence of this phenomenon upon diffusion is negligible.

Finally we considered the diagonal elements of the SDT for decane. The functional dependence of these elements upon the shear rate, which is depicted in Fig. 6, seems to be something intermediate between that of the GB fluid and CS_2. The behavior of the *xx* element seems to be very similar to that of the same quantity for the GB fluid. It is obviously closely related to the order parameter, shown in Fig. 3(a). It is evident from Fig. 3(b) that the alignment angles of the order tensor and the SDT are also fairly well correlated but the alignment angle of the pressure tensor behaves differently.

It should also be noted that, unlike CS_2 and the GB fluid, decane molecules change their shape as the shear rate increases. The radius of gyration initially increases, reaching a maximum at $\gamma\tau=0.60$ and then it decreases. The decrease of D_{xx} at higher shear rates can be attributed to higher pressure and increasing rotational temperature. Contrary to the case of the GB fluid, D_{yy} and D_{zz} grow with γ and they do not decrease until the shear rate becomes very high. This is similar to CS_2. By studying the diagonal VACF's, shown in Fig. 7, one finds that the equilibrium correlation functions are negative after the initial positive contribution has decayed. This negative region is fairly long and shallow so it is quite different

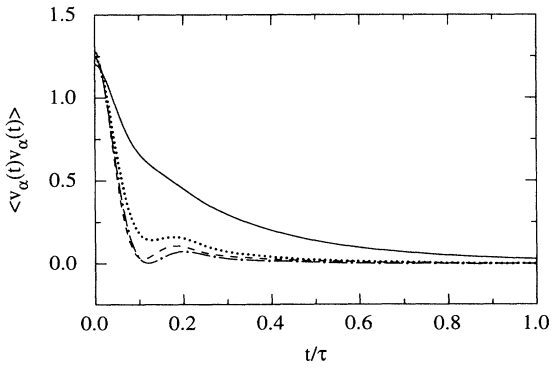

FIG. 5. Diagonal velocity autocorrelation functions, $Z_{\alpha\alpha}(t)=\langle v_\alpha(t)v_\alpha(0)\rangle$ of the GB fluid. The full curve, the dashed curve, and the dash-dotted curve denote $Z_{xx}(t)$, $Z_{yy}(t)$, and $Z_{zz}(t)$ at a reduced shear rate of 1.0. The dotted curve is the equilibrium velocity autocorrelation function.

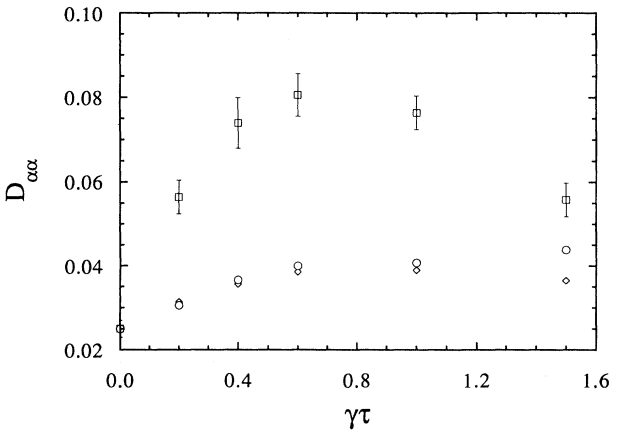

FIG. 6. As in Fig. 1 but the system is decane.

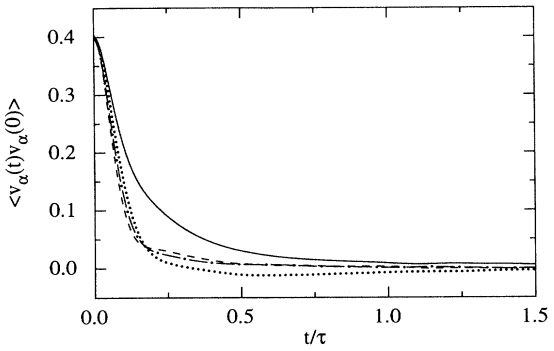

FIG. 7. Diagonal velocity autocorrelation functions, $Z_{\alpha\alpha}(t)=\langle v_\alpha(t)v_\alpha(0)\rangle$ of decane. The full curve, the dashed curve, and the dash-dotted curve denote $Z_{xx}(t)$, $Z_{yy}(t)$, and $Z_{zz}(t)$ at a reduced shear rate of 0.60. The dotted curve is the equilibrium velocity autocorrelation function.

from the VACF of CS_2 or a LJ fluid. However, the result is the same, namely, to decrease the GK integral and thereby the diffusion coefficient. At higher shear rates this negative region vanishes and D_{yy} and D_{zz} are enhanced. This is different from the GB fluid where the *yy* and *zz* VACF's develop backscattering features at high shear rates. The difference is presumably due to the flexibility of the decane molecule. Collisions are softened by internal relaxation, and this "shock absorber" effect may be enhanced at high shear rates, where dihedral angle transition rates are far higher than they are at equilibrium. The *xx* VACF of decane is very similar to that of the GB fluid. The decay time of $\langle v_x(t)v_x(0)\rangle$ increases as the system becomes more ordered and the alignment angle of the order tensor decreases to about 20°.

One of the major differences between the SDT of a shearing system and that of an equilibrium system is that the D_{xy} and the D_{yx} elements of the diffusion tensor are nonzero. This means that a concentration gradient of labeled particles in the *x* direction can drive a current in the *y* direction and vice versa. We have found that the functional dependence of these elements upon the shear rate for the three different systems studied in this work is very similar so we discuss them at the same time. The off-diagonal elements are depicted in Fig. 8 as functions of γ, for CS_2 [Fig. 8(a)], GB [Fig. 8(b)], and decane [Fig. 8(c)]. The behavior of D_{xy} and D_{yx} of decane and the GB fluid is very similar at low shear rates. They are nearly equal and positive. As the shear rate grows D_{xy} becomes larger than D_{yx} and they both pass through a maximum. After this, D_{yx} falls off very rapidly and eventually becomes negative. In the GB fluid D_{xy} follows D_{yx} in the rapid decline whereas D_{xy} in decane diminishes more slowly and remains positive. The diffusion tensor of decane is thus highly asymmetric at high shear rates and the off-diagonal components eventually have different signs. In CS_2 the off-diagonal elements are also equal and positive at low shear rates. At higher shear rates D_{xy} of CS_2 behaves like D_{yx} of decane. Conversely, we have found that D_{yx} of CS_2 behaves like D_{xy} of decane. The element D_{xy} is consequently smaller than D_{yx} and it finally becomes negative while D_{yx} remains positive. At high shear rates, the SDT of CS_2 is thus a mirror image of the SDT of decane.

As in the case for the diagonal elements of the SDT we can obtain some further understanding by studying the off-diagonal VACF's, $\langle v_x(t)v_y(0)\rangle$ and $\langle v_y(t)v_x(0)\rangle$. In the systems and state points studied in this work the cross correlation functions have a very rich structure.

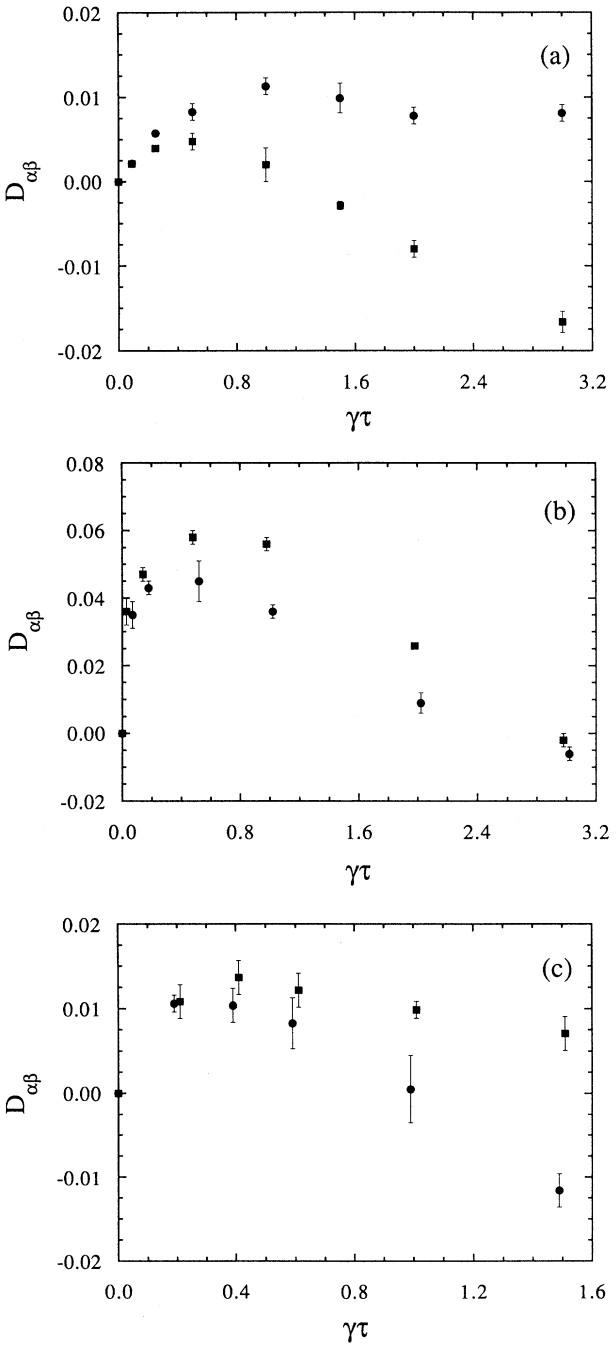

FIG. 8. The off-diagonal elements of the SDT of (a) CS_2, (b) the GB fluid, and (c) decane as functions of the shear rate. The filled squares depict D_{xy} and the filled circles depict D_{yx}.

There are many events that together are responsible for the exact features of the correlation functions. It is very hard to identify all of these events and their relative contribution so we will only point out a few effects that are consistent with the observed structures. The simplest behavior of these two quantities can be seen in the low-density limit. Then it is possible to obtain the signs of D_{xy} and D_{yx} from the cross-correlation functions. It is also possible to discern some remnants the low-density behavior at higher densities. Therefore we have included some low-density data, $n\sigma_0^3=0.10$, $k_BT/\varepsilon_0=1.25$, and $\gamma\tau=0.20$, for the off-diagonal VACF's of the GB fluid. As one can see in Fig. 9, they are negative at time zero and they decay monotonically to zero. They are essentially similar to those of a low-density LJ fluid.

At low densities the time between collisions is fairly long so the molecules can travel relatively long distances without being impeded. Keeping this in mind it is easy to realize that $\langle v_x(0)v_y(0)\rangle$ must be negative. If $v_y(0)$ is positive, the molecule must have been moving in the positive y direction since the last collision at some time $-t_0$. When the molecule moves in this direction the local streaming velocity, $u_x(y)$, increases. If the molecule does not collide with any other molecules the laboratory velocity $\dot{r}(t)$ in the x direction does not change and the peculiar velocity $v_x(t)=\dot{r}(t)-u_x(y)$ becomes smaller and smaller. If we assume that the expectation value of $v_x(t)$ after the collision at $-t_0$ is zero, then it is more likely that $v_x(0)$ is negative than that it is positive. Thus $\langle v_x(0)v_y(0)\rangle$ is negative. At low densities the correlation function decays monotonically to zero, so the corresponding GK integral and the off-diagonal diffusion coefficient is negative. This conclusion has also been confirmed for a low-density LJ fluid in Ref. [8].

If we look at the cross-correlation functions at low shear rates, shown in Figs. 10(a)–10(c) we find that the time zero value is very close to zero, which means that $v_x(0)$ and $v_y(0)$ are very nearly uncorrelated. This implies that the observed time zero velocities are mainly the result of random collisions. The very slight negative value shows that there are still some very short free flights between the collisions. The large positive peak of $\langle v_x(t)v_y(0)\rangle$ and $\langle v_y(t)v_x(0)\rangle$ imply that an initial positive $v_x(0)$ is fairly likely to yield a large $v_y(t)$ a short time later and vice versa. It is these peaks that make D_{xy} and D_{yx} positive at low shear rates. Since those peaks are

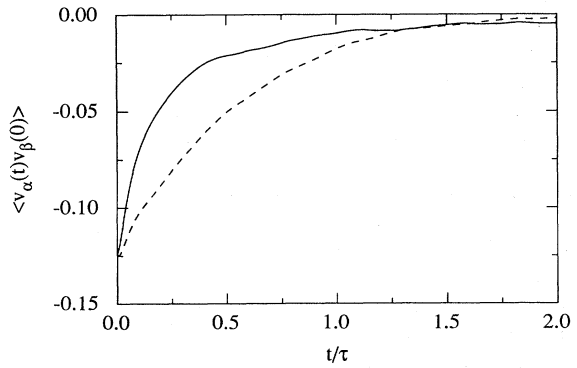

FIG. 9. Off-diagonal velocity autocorrelation functions, $Z_{\alpha\beta}(t)=\langle v_\alpha(t)v_\beta(0)\rangle$ of the GB fluid at low density. The full curve denotes $Z_{xy}(t)$ and the dashed curve denotes $Z_{yx}(t)$ at a reduced shear rate, density and temperature of 0.20, 0.10 and 1.25.

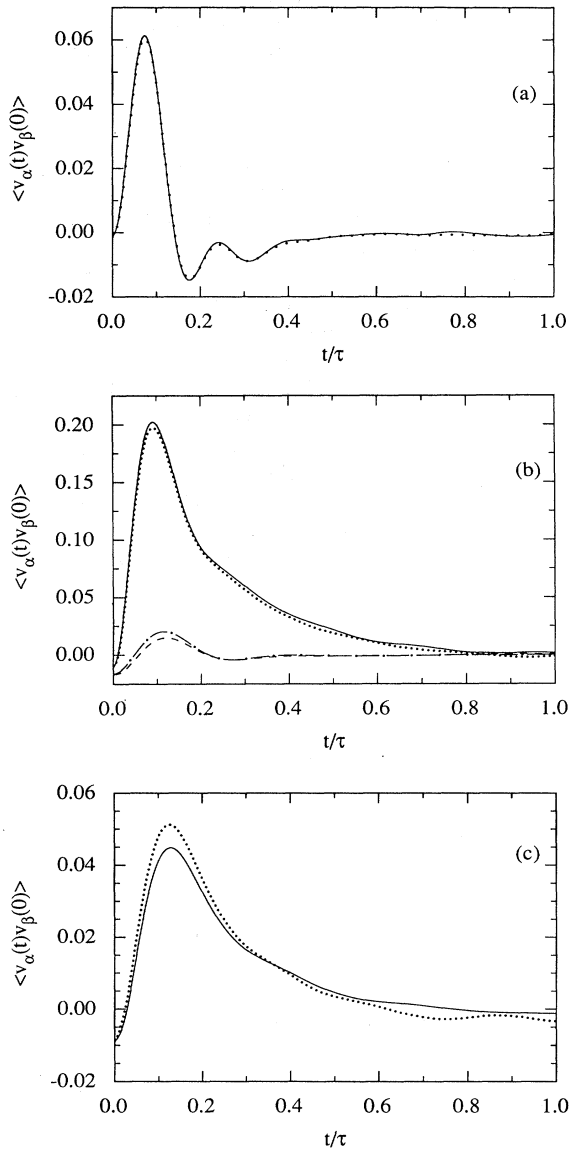

FIG. 10(a). Off-diagonal velocity autocorrelation functions, $Z_{\alpha\beta}(t)=\langle v_\alpha(t)v_\beta(0)\rangle$ of CS_2. The full curve denotes $Z_{xy}(t)$ and the dashed curve denotes $Z_{yx}(t)$ at a reduced shear rate of 0.090. (b) Off-diagonal velocity autocorrelation functions, $Z_{\alpha\beta}(t)=\langle v_\alpha(t)v_\beta(0)\rangle$ of the GB fluid. The full curve denotes $Z_{xy}(t)$ and the dashed curve denotes $Z_{yx}(t)$ at a reduced shear rate of 0.090. The dash-dotted and the dashed curves represent $Z_{xy}(t)$ and $Z_{yx}(t)$ of a triple-point Lennard-Jones fluid at a reduced shear rate of 0.16. (c) Off-diagonal velocity autocorrelation functions, $Z_{\alpha\beta}(t)=\langle v_\alpha(t)v_\beta(0)\rangle$ of decane. The full curve denotes $Z_{xy}(t)$ and the dashed curve denotes $Z_{yx}(t)$ at a reduced shear rate of 0.20.

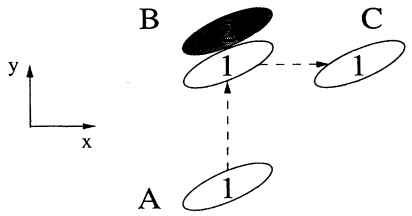

FIG. 11. A possible collision sequence that could account for the positive peak of the off-diagonal velocity autocorrelation functions at low shear rates. Particle 1 starts at A at time zero. A short while afterwards it collides with particle 2 at B and is deflected towards C.

much larger in the fluids consisting of rodlike molecules than in a high-density Lennard-Jones fluid, the cross-correlation functions of which are included in Fig. 10(b), we believe that the alignment of the molecules plays a significant role in the generation of those peaks.

In Fig. 11 we sketch a "collision" sequence that could explain why the alignment causes positive peaks in $\langle v_y(t)v_x(0)\rangle$ and $\langle v_x(t)v_y(0)\rangle$ at short times. We assume that there is some space left between the molecules. If we follow one molecule with positive velocity in the y direction at time zero, it will soon collide with another molecule which is oriented parallel to itself, i.e., at angle between 15°–45° to the streamlines. During this collision some of the positive velocity in the y direction is deflected in the positive x direction. This type of collision gives a

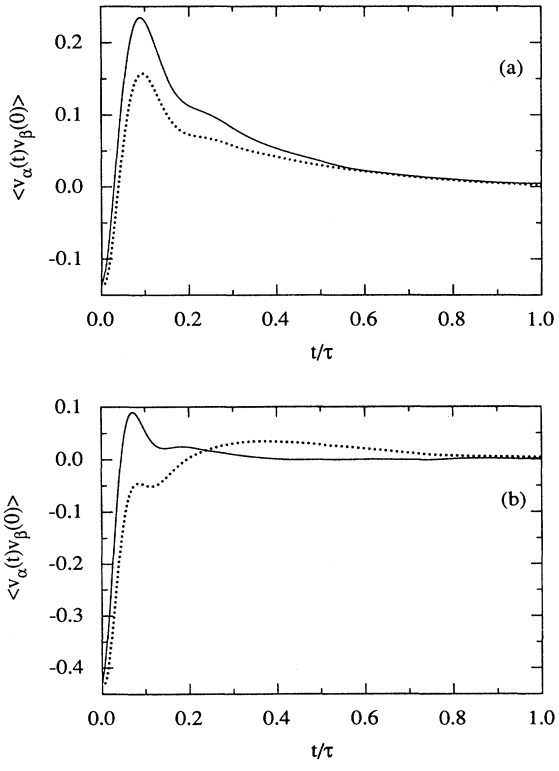

FIG. 12(a). As in Fig. 10(b) but the reduced shear rate has been increased to 1.0. (b) As in Fig. 10(b) but the reduced shear rate has been increased to 3.0.

positive contribution to $\langle v_x(t)v_y(0)\rangle$ at short times. In a similar way one can argue that $\langle v_y(t)v_x(0)\rangle$ gets a positive contribution at short times.

Finally, for the sake of completeness we have included two high shear rate results for the cross-correlation functions of the GB fluid. In Figs. 12(a) and 12(b) we show these functions for $\gamma\tau=1.0$ and 3.0. At first the time zero value becomes more negative and it approaches the same magnitude as the positive maximum. The cross-correlation functions thus become more similar to those of a dense Lennard-Jones fluid [8]. At the highest shear rates the two off-diagonal correlation functions differ from each other more and more. The positive region diminishes or vanishes completely. They also become much less structured. This disappearance of structure may be due to the increasing rotational temperature. However, when $\gamma\tau>1.0$ the difference between the rotational and translational temperatures becomes dependent on the details of the thermostatting mechanism employed in the simulation. It is consequently very hard to draw any definite conclusions about the behavior at high shear rates.

IV. CONCLUSIONS

We have studied self-diffusion under shear for three different model fluids, namely, the Tildesley-Madden model for carbon disulfide, the Ryckaert-Bellemans model for decane, and the Gay-Berne fluid. We have found that two different mechanisms are responsible for the functional dependence of the diagonal elements of the SDT upon the shear rate. The first one is basically the same as the one found in dense Lennard-Jones fluids [4,8]. In a dense fluid every molecule is surrounded by a shell of nearest neighbors. Whenever a molecule moves, it is very likely to collide with another molecule in the shell. This greatly impedes diffusion. When the shear rate is high, the coordination shell is distorted. Then it becomes easier for a molecule to penetrate the long axis of the nearest-neighbor cage and the movement of the molecules is greatly facilitated. This enhances diffusion in this direction. This mechanism has been found to be particularly important in carbon disulfide. The xx element of the diffusion tensor increases by a factor of 40. The reason for this is probably that the diffusion coefficient is very low to begin with, because of a particularly rigid cage structure at equilibrium.

In the nonlinear shear rate regimes that we have studied the angle between the principal axis of the order tensor and the streamlines has decreased from the linear value of 45° to between 15° and 25°. This facilitates diffusion in the direction along the principal axis of the order tensor. Diffusion in the direction perpendicular to the principal axis is impeded because the molecules must move sideways in that direction. This mechanism seems to explain the behavior of the diagonal elements of the SDT of the GB fluid under shear.

The functional dependence of the xx element of the SDT upon shear on all three fluids discussed here seems to be correlated with the functional dependence of the or-

der parameter upon the shear rate. The alignment angle of the order tensor and the traceless symmetric part of the SDT also agree fairly well at low shear rates, $\gamma\tau < 1.0$. At higher shear rates they diverge. The shear rate dependence of the alignment angle of the symmetric traceless pressure tensor is different from that of the other two tensors.

We have found that the period of the shear induced rotation is far longer than the convergence time of the Green-Kubo integrals for the various elements of the SDT. Shear induced rotation consequently does not affect diffusion very much.

A major difference between the equilibrium SDT and the SDT of a shearing fluid is that the xy and yx elements of the latter system are nonzero. We have found an argument why these elements should be negative at low densities, both for molecular and atomic fluids. Our simulation results indicate that this is indeed the case. This is very different from the high-density results. Then the off-diagonal elements of the SDT for a Lennard-Jones fluid are almost zero but those of the molecular fluids in this study are positive. We found that this is due to a very large peak in the velocity cross-correlation function at time $t = 0.1\tau$. It is possible that this large peak is due to a certain kind of collision that becomes possible when the molecules are strongly aligned. At low shear rates D_{xy} and D_{yx} are equal within the statistical uncertainties but as the shear rate increases they become more and more unequal and may even have opposite signs. The SDT is then highly asymmetric.

Finally we note that in order to obtain measurable changes of the SDT the shear rate must be of order one in reduced units for decane and the GB fluid and order 0.10 for CS_2. These high shear rates are hard to realize in a laboratory for decane or CS_2. In order to see nonlinear behavior experimentally one could more easily study colloidal systems or fluids consisting of rodlike polymers. In these systems the nonlinear regime is more accessible.

[1] S. R. de Groot and P. Mazur, *Nonequilibrium Thermodynamics* (Dover, New York, 1984).
[2] D. J. Evans and G. P. Morriss, *Statistical Mechanics of Nonequilibrium Liquids* (Academic, London, 1990).
[3] D. M. Heyes, J. J. Kim, C. J. Montrose, and T. A. Litovitz, J. Chem. Phys. **73**, 3987 (1980); D. M. Heyes, J. Chem. Soc. Faraday Trans. 2 **82**, 1365 (1986).
[4] P. T. Cummings, B. Y. Wang, D. J. Evans, and K. J. Fraser, J. Chem. Phys. **94**, 2149 (1991).
[5] S. Sarman, D. J. Evans, and P. T. Cummings, J. Chem. Phys. **95**, 8675 (1991).
[6] D. J. Evans, Phys. Rev. A **44**, 3630 (1991).
[7] D. J. Evans, A. Baranyai, and S. Sarman, Mol. Phys. **76**, 661 (1992).
[8] S. Sarman, D. J. Evans, and A. Baranyai, Phys. Rev. A **46**, 893 (1992).
[9] J. G. Gay and B. J. Berne, J. Chem. Phys. **74**, 3316 (1981).
[10] D. J. Tildesley and P. A. Madden, Mol. Phys. **42**, 1137 (1981); **48**, 129 (1983).
[11] J. P. Ryckaert and A. Bellemans, Discuss. Faraday Soc. **66**, 95 (1978).
[12] E. de Miguel, L. F. Rull, M. K. Chalam, K. E. Gubbins, and F. van Swol, Mol. Phys. **72**, 593 (1991).
[13] E. de Miguel, L. F. Rull, M. K. Chalam, and K. E. Gubbins, Mol. Phys. **71**, 1223 (1990); **74**, 405 (1991).
[14] M. K. Chalam, K. E. Gubbins, E. de Miguel, and L. F. Rull, Mol. Sim. **7**, 357 (1991).
[15] E. de Miguel, L. F. Rull, and K. E. Gubbins, Phys. Rev. A **45**, 3813 (1992).
[16] D. J. Evans, Mol. Phys. **34**, 317 (1977).
[17] R. Edberg, D. J. Evans, and G. P. Morriss, J. Chem. Phys. **84**, 6933 (1986); **86**, 4555 (1987).
[18] P. J. Daivis, D. J. Evans, and G. P. Morriss, J. Chem. Phys. **97**, 616 (1992).
[19] G. P. Morriss, P. J. Daivis, and D. J. Evans, J. Chem. Phys. **94**, 7420 (1991).
[20] R. Edberg, D. J. Evans, and G. P. Morriss, Mol. Phys. **62**, 1357 (1987).
[21] S. Y. Liem, D. Brown, and J. H. R. Clarke, Phys. Rev. A **45**, 3706 (1992).